Bond behavior of Concrete Beam Reinforcement by GFPR Bars

Hamdy Kamal Shehab eldin, Mohamed Hussein, Khaled Fawzy and Shady Khairy.

Structural Engineering Department, Faculty of Engineering, Zagazig University, Egypt.
khaled_lashen1@yahoo.com

Abstract: In recent years, some attempts have been performed to extend general design rules reported in the codes for steel reinforced concrete to Fiber Reinforced Polymer (FRP) materials; this is the case of relationships adopted in the evaluation of the development length clearly derived by extension of the formulations used for steel bars. However, such relationships seem to be inappropriate for FRP reinforcing bars: in fact, experimental test results have shown that bond behavior of FRP bars is different from that observed in case of deformed steel ones. As a consequence, a new procedure for the evaluation of development length based on an analytical approach is needed in order to directly account for the actual bond-slip constitutive law as obtained by experimental tests on different types of FRP reinforcing bars. During this research contribution, an experimental study of GFRP bar concrete bond test is carried out and presented to investigate the bond stress–slip behavior for normal and fiber concrete. The tested specimens included 19 concrete beams by 1200mm as a length, 200mm as a width and 100mm as height .The GFRP bars embedded in concrete beams by embedded length equal 100mm and 250mm.This research effort aims at underlining the effects of embedded length of (GFRP), the fiber, and the dynamic load on the maximal bond stress.
[Hamdy Kamal Shehab eldin, Mohamed Hussein, Khaled Fawzy and Shady Khairy. **Bond behavior of Concrete Beam Reinforcement by GFPR Bars**. *Life Sci. J* 2014; 11(11):113-123] (ISSN: 1097-8135). http://www.lifesciencesite.com 15

Keywords: R C beams, Bond, Embedded length, Fiber reinforced polymers; FRP, Tension stiffening.

1. Introduction

Considerable research efforts have been conducted on the bond behavior of glass fiber reinforced plastic (GFRP) rebar in concrete. Different types of FRP bars have quite different bond characteristics, which are strongly dependent on developed length, mechanical and physical properties of external layer of FRP rods. [1,19]

In order for FRP bars to become widely accepted in the construction industry, all aspects of their structural behavior must be studied to guarantee their safe application. Bond development is a critical issue for their successful application as reinforcement in concrete structures. Bond characteristics affect the anchorage of bars, strength of lap splices, required concrete cover, and serviceability and ultimate states. The continued integrity of the bond is also a critical issue for the long lasting performance of concrete structures reinforced with FRP bars. [2, 4, 17 and 18]

Bond strength of fiber reinforced polymer (GFRP) bars was experimentally investigated in this study and compared to that of steel bars. A total of 19 concrete beams reinforced with two types of bars, GFRP bars and steel bars were tested. The type of concrete is a parameter with the research, which a total 19 concrete beam can classified for (NC) normal concrete and (FC) fiber concrete. Diameter of GFRP and steel bars with 10 mm, and two embedment lengths (Ld), 100mm, and 250mm were used. All specimens tested by 4-point bending test to descried bond stress and slippage of bars.

2. Experimental Work

In this research, The beams were instrumented and tested under four-point bending condition (4PB) with different types of reinforcements, steel and fiber glass (GFRP) bars to determine a clear comparative between reinforcement by steel and GFRP in two types of normal concrete concrete (NC), concrete fiber (FC) and clarify the bond behavior between the bars and the concrete used.The deformed steel bars are used to provide reference for comparison of results. The objectives of this study are to investigate experimentally the bond-slip behavior between concrete and GFRP reinforcing bars under static and dynamic loading with different (Ld) for both steel normal concrete (NC), steel fiber concrete (FC), GFRP normal concrete (NC) and GFRP fiber concrete (FC). The beam specimens are tested under static and cycling loading to describe the bond stress and the slippage which occurs in bar, and concrete.

2.1 Bond test specimen

The specimens tested included 9 beams with embedded length (Ld) equal 100mm, and 10 beams with embedded length (Ld) equal 250mm, both of them reinforced by GFRP bars and steel bars .Type of concrete is a very important parameter which was classified for two types of concrete, (NC) normal concrete, and (FC) fiber concrete. Concrete dimension of 19 beams are 200mm height, 100mm width, and 1200mm Length. Concrete was poured in the mold beam after placing GFRP, Steel bars as shown in Figure .3. Developed length is the embedded length of bar into concrete as shown in Fig. 4. For Manufacture processing and casting concrete beam were finished in laboratories of Higher Technological institute 10th of Ramadan, Testing process was occurred in laboratories of Structural Engineering Department, Zagazig University by MTS machine, with Capacity 200KN.Specimens were tested as 4-piont bending test to describe stress-strain curve and calculate modulus of elasticity as shown in Figure1, the developed length, which is the embedded length of bar into concrete is shown in Fig. 2. Three different surface treatments are applied to the manufactured GFRP bars. First type has spirally wrapped fiber strand with pitch of about 25.4 mm, and helically rounded with about 45° degrees to the longitudinal direction. The second type is coated by sand (sanded). The last type was left untreated with cleaning the bar surface from any increases of resin to make it completely smooth. Mechanical bond was also added to some bars by providing an enlargement to the bar ends. Table (1) shows the details of concrete beams that have been tested by the surface texture as well as the developed length of the different reinforcing bars used in the experimental program. The properties of (FC) are shown in table (2).

Fig.1 Beam Test on specimens by MTS machine capacity 200KN

Table (1) the details of concrete beams tested

Beam	NC or FC	Bar Surface	Bar type	Bond length (L_d) mm
B1	NC	Mech.	GFRP	100
B2	NC	Spiral	GFRP	100
B3	FC	Sanded	GFRP	250
B4	FC	Sanded	GFRP	250
B5	NC	Mech.	GFRP	250
B6	NC	Sanded	GFRP	100
B7	NC	Sanded	GFRP	100
B8	NC	H.G.S	Steel	250
B9	NC	H.G.S	Steel	100
B10	NC	H.G.S	Steel	250
B11	NC	H.G.S	Steel	100
B12	FC	H.G.S	Steel	250
B13	FC	Sanded without stirrups	GFRP	100
B14	FC	H.G.S	Steel	100
B15	NC	Spiral	GFRP	250
B16	FC	Sanded	GFRP	100
B17	FC	H.G.S	Steel	250
B18	NC	Smooth	GFRP	100
B19	NC	Smooth	GFRP	250

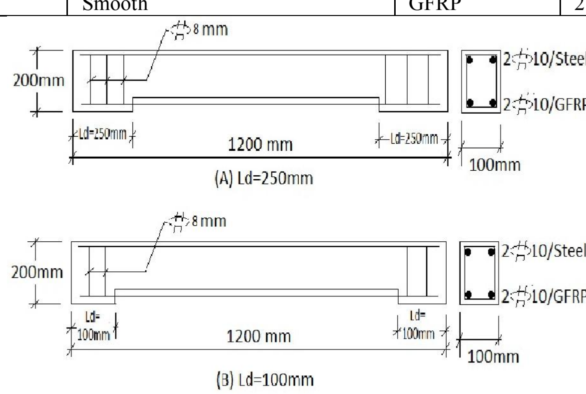

Fig. 2 Concrete beams that have been tested

Fig.3 The mold beam which concrete was poured

Table (2) the properties of the used concrete

Fiber reinforced concrete (FC.)					
Gravel **Kg/m^3**	***Sand*** **Kg/m^3**	***Cement*** **Kg/m^3**	***Water*** **lit/ Kg/m^3**	***Fiber*** **Kg/m^3**	***Super plastizer*** **Kg/m^3**
1026	**790**	**390**	**195**	**2.7**	**1.5% of Cement**

Fig. 4 Developed length is the embedded length of bar into concrete

2.2 Materials

The following materials were used in concrete mix: **Aggregates:** Natural siliceous sand was used as Fine aggregate, with properties and grading curve as shown in table 3 and Fig. 5 respectively. Dolomite with nominal maximum size of 14 mm is used as coarse aggregate. Sieve analysis of dolomite is given in Fig. 6. The dolomite is washed twice with clean drinking water, and immersed in water to be fully saturated and then left to dry in the room temperature before mixing.

Table (3) Physical properties of fine aggregates

Property	Measured Value	Code Limits
Compacted density	1725 Kg/m3	
Loose density	1600 Kg/m3	
Specific gravity	2.65	2.5 – 2.75
Fine material < (75 µ)	1.0 %	up to 3%

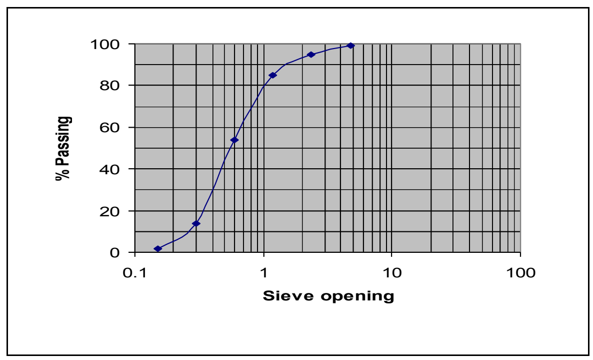

Fig.5. Grading curve of sand

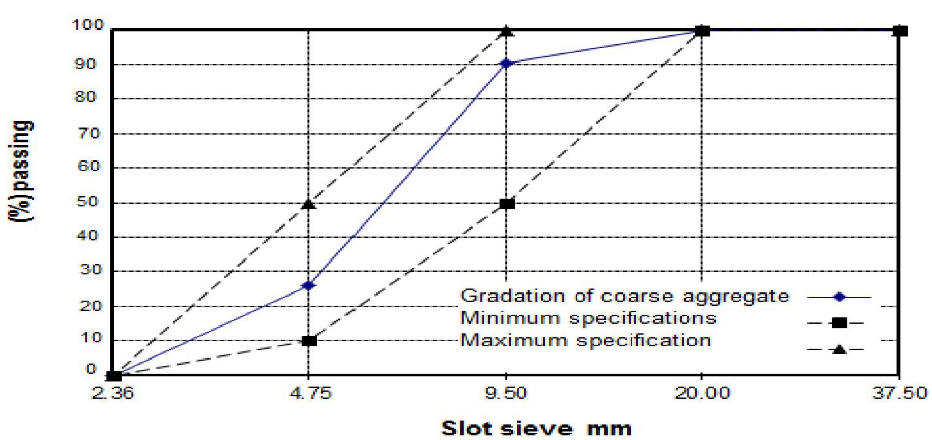

Fig. 6 grading curve of dolomite

Cement: ASTM Type1 Ordinary Portland cement (N42.5) is used in this work.

Water: Tap water was used. The water-cement ratio is taken constant in all mixes and equals to 0.48.

Polypropylene fibers: For practical application, the volume fraction (V_f) of 0.3% (about 2.7 kg/m^3) of polypropylene fibers was used in fiber concrete (FC). This ratio allows taking the benefits of fibers, while ensuring appropriate workability of concrete. It should be noted that the one of the objectives of this study is to qualitatively investigate the benefits gained from adding fibers to the bond strength of GFRP reinforcing bars. The compression strength of concrete on the day of testing was 27 MPa and 30 MPa for FC and plain concrete NC, respectively.

Reinforcement

Two types of reinforcement were used in the specimens, steel bars in reference specimens and GFRP bars in the other specimens as shown in Fig. 7.

Steel bar **(a) Before coating (Smooth)** **(b) After coating**

Fig.7 Steel bar and GFRP Bar ϕ10mm

Bar surface texture

The shapes of the type of GFRP reinforcing bars are shown in Fig. 7. Bars having a length of 1200mm and nominal diameter of 10 mm were produced using 70% E-glass fiber and 30% a polyester resin. The GFRP bars manufacturing process according to Safaan (2004) [15] is used in this research. Three different surface treatments are applied to the manufactured GFRP bars. First type has spirally wrapped fiber strand with pitch of about 25.4 mm, and helically rounded with about 45° degrees to the longitudinal direction. The second type is coated by sand (sanded). The last type was left untreated with cleaning the bar surface from any increases of resin to make it completely smooth. Mechanical bond was also added to some bars by providing an enlargement to the bar ends. Stress-Strain curve of the reinforcing GFRP, and steel bars used in the test specimens is schematically shown in Fig. 8. The average elastic modulus of GFRP (E_g) is found to be about 0.23 of the elastic modulus of steel (E_s),where the modulus of elasticity of steel bar was found equal 200000 MPa. [18].

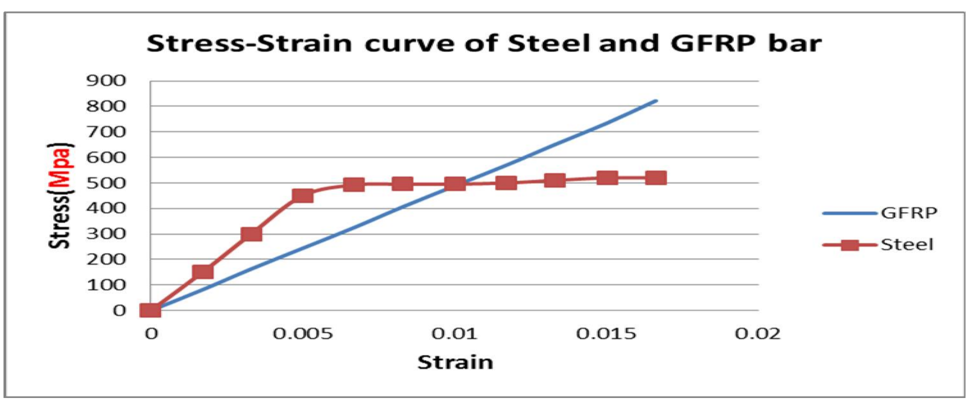

Fig 8.Stress-Strain curves of GFRP bar and steel bar

3. Beam Tests

It is the commonly used test procedure to evaluate the bond behavior. It is an economic and simple test procedure for the evaluation of bond performance [16, 17].

Linear vertical displacement transducers (LVDT) were used to measure the machine displacement increment, while strain gauges were mounting on the bar to measure its strain. Piece of rubber with thickness 10mm was placed between concrete beam and supporting steel block to prevent bending or movement due to the irregularities at the contact surface of the beam. The beam tests were carried out on the MTS machine at Concrete Lab at Faculty of Engineering, Zagazig University, Egypt. The setup of the beam test is shown in Fig. 9. Displacement control Load was applied. The maximum capacity of the MTS machine is 200 KN. descriptions of nineteen beam specimens are shown in Table 1.

Fig.9. the schematic arrangement of the beam test on MTS 200KN as a capacity

4. Bond Test Results

The specimens were tested under four point bending (4-PB) up to failure. The deflection was measured at the bottom of middle span of the beam. Load-Deflection curves of the tested specimens are plotted in Figs. 10, 11, 12, 13, and 14. Also; Table 4 shows the ultimate load and the corresponding deflection at middle span of the tested specimens. The failure shapes of beam specimens are shown in Fig. 10, in all specimens, failure diminishing of load carrying capacity took place at maximum load just after the Longitudinal splitting cracks started near the support except the specimens B3 and B10, the specimen B3 failed in compression failure with losses in its ultimate load due to the property of existence of voids in fiber concrete. The specimen B10 is reached to the ultimate load with vertical cracks at the tension zone and finally compression failure occurred.

(a) Steel bar **(b) GFRP bar**

Fig.10. Failure mode for reinforcement concrete beams by Steel bar and GFRP bar

Table 4: Load-Deflection of tested beams

Beam	NC or FC	Bar Surface	Bar	L_d mm	P_u KN	Δ_u mm	Failure mode
B1	NC	Mechanical	GFRP	100	18	3.91	Bond
B2	NC	Spiral	GFRP	100	15	8.5	Bond
B3	FC	Sanded	GFRP	250	42	8.8	compression
B5	NC	Mechanical	GFRP	250	51.4	12	compression
B6	NC	Sanded	GFRP	100	8	9.5	Bond
B7	NC	Sanded	GFRP	250	35	5.4	Bond
B10	NC	notched	Steel	250	47	8.9	compression
B15	NC	Spiral	GFRP	250	48.8	9.75	compression
B16	FC	Sanded	GFRP	100	12	2.71	Bond
B17	FC	notched	Steel	250	32	1.82	Bond

4.1 Load-Deflection for Normal Concrete

Fig. 11 shows the load-deflection curves of the specimens B1 and B5, both of them have mechanical GFRP bars with embedded length 100 mm and 250mm respectively, the specimen B1 failed at 18 KN with bond failure and the corresponding deflection was 3.91mm, the ultimate load failure of the specimen B5 increased up to 51.4 KN with deflection 12mm. the failure mode was changed to compression failure with increasing embedded length, it can be clearly observed in table 4, which as the embedded length increased, the ultimate failure load increased.

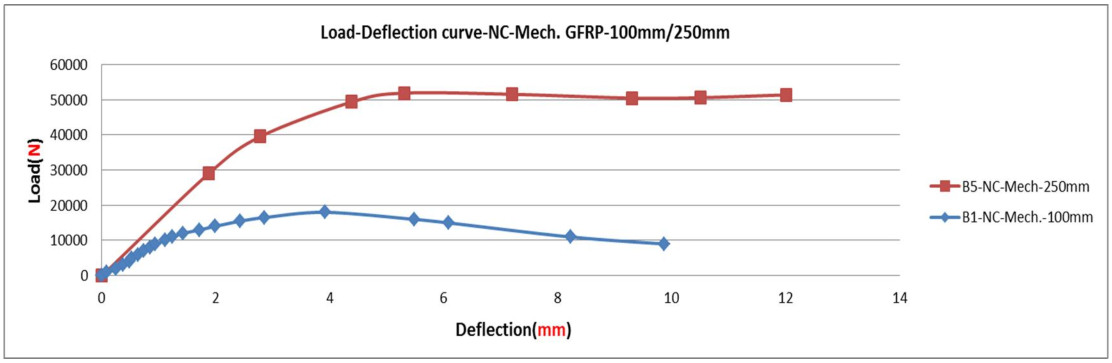

Fig.11. Load-Deflection experimental behavior of GFRP B1 and B5

4.2 Load-Deflection for Fiber Concrete

Figs. 12 and 13 show the load-deflection behavior of specimens B6, B7 (normal concrete) and specimens B16, B3 (fiber concrete) respectively with same treatment of bars surface (sanded surface). From observation, the embedded length and the surface treatment have significant effect in enhanced the failure load, the failure loads for B7and B3 reached to 35, 42 Kn respectively (with embedded length 250 mm), the fiber concrete increased the ultimate load by about 16%, and enhanced the failure mode from bond failure to compression failure. Regardless of the concrete type, the fiber concrete has the little effect in increasing the ultimate load or enhanced the failure mode for specimen with 100 mm embedded length.

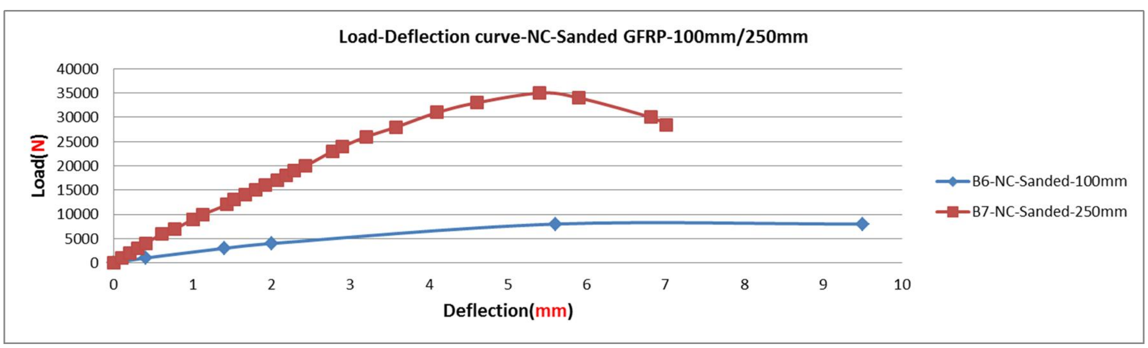

Fig.12. Load-Deflection experimental behavior of GFRP B6 and B7

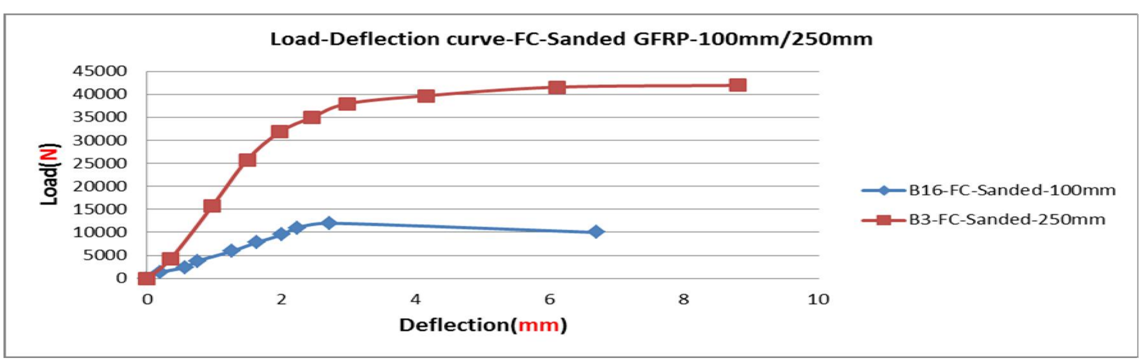

Fig.13. Load-Deflection experimental behavior of GFRP B16 and B3

Fig. 14 shows the load-deflection behavior of specimens (B2 and B15), both of them have spiral GFRP bars with embedded length 100 mm and 250mm respectively. The specimen B2 failed at 15 KN with bond failure and the corresponding deflection was 8.5mm, the ultimate load failure of the specimen B15 increased up to 48.8 KN with deflection 9.75mm, the behavior is the same as the specimens with mechanical treatment.

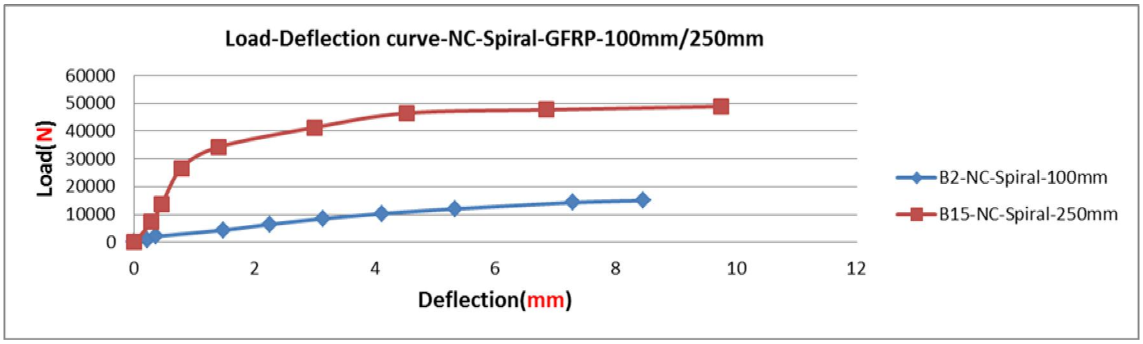

Fig.14. Load-Deflection experimental behavior of GFRP B2 and B15

As can be seen from the above Figures, the beam specimens with embedded length 250 mm had greater stiffness than did by the beam specimens with embedded length 100 mm, due to the increasing of bond resistance.

Fig. 15 shows the load-deflection behavior of B7,B3, B5 and B15 with embedded length 250mm by different surface treatment comparing with specimen B10 (notched steel bar) as a reference. The Specimen B10 reached to ultimate load capacity 47 KN with final compression failure, however the specimen B7 (sand normal concrete surface treatment), the failure load is found to be lower than B10 by about 25%, while the specimen B3 is found to be lower than B10 by about 10%. Both of specimens have not reached to the optimum failure load. For the specimen B15 (spiral normal concrete surface treatment), and the specimen B5 (mechanical normal concrete surface treatment), the failure loads are found to be higher than B10 by about 3%and 9 % respectively, this means that, both treatments give the maximum bond strength for GFRP bars. The initial bond stiffness of GFRP specimens is similar to bond stiffness of the deformed steel initial bond stiffness, and after cracking load, there were differences between the stiffnesses of all beam specimens, the sand bond (B7) has the minimum stiffness compared to the other treatment specimen.

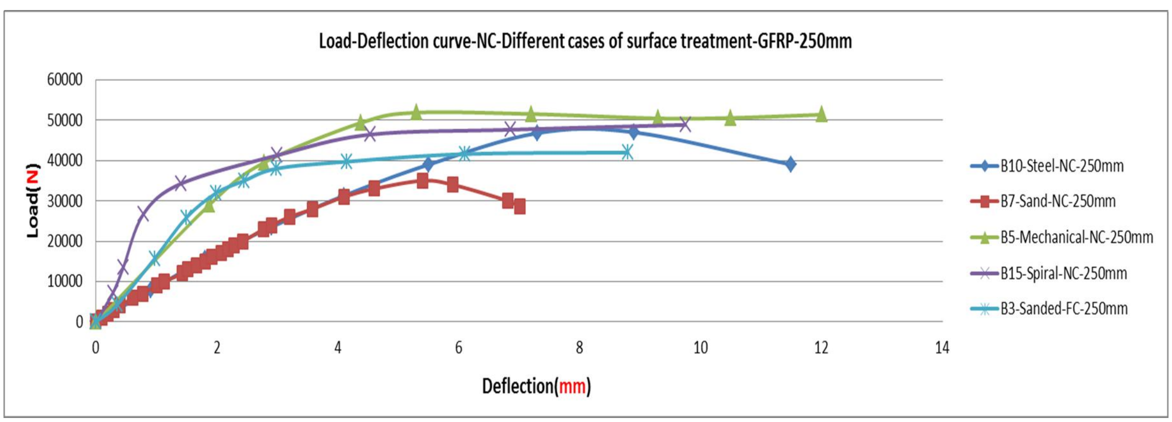

Fig.15. Load-Deflection experimental behavior of GFRP beam B10, B7, B5 and Steel beam B15

4.3 Bond and Slip Calculation

The bond-slip experimental behavior of the beams is drawn in Figs. 17, 18, 19, 20, and 21, the equations. (1), (2), (3), (4) and (5) are used to obtain the ultimate values of bond stress and bar slippage for different specimens. The results of calculations are shown in table 5.

$$a = \frac{110-24}{2} = 43\ cm \quad \text{Moment, } M = \frac{P \times a}{2}$$

$$d = t - cover = 20 - 2.5 = 17.5\ cm$$

$$T_i = \frac{M}{0.87 \times d} = 1.43 \times P_i \quad \ldots\ldots\ldots\ldots Eq(1)$$

$$T_i = \varepsilon_i \times E \times Area\ of\ one\ bar \quad \ldots\ldots\ldots\ldots Eq(2)$$

Area of one bar = $\pi \times \emptyset^2 / 4$

Elongation, $\Delta L_i = \varepsilon_i \times (L_1 + L_d) \quad \ldots\ldots\ldots\ldots Eq(3)$

Slippage, $S = \delta_i - \Delta L_i$ ....$Eq(4)$

Bond stress, $\tau = \frac{T_{ave.}}{\pi \times \emptyset \times L_d} \quad \ldots\ldots\ldots\ldots Eq(5)$

$T_{ave.}$ Average value between T_i from equ. (1) and T_i from equ.(2)

T_i Tension force of one bar

δ_i Horizontal experimental value due to strain gauges

ε_i Experimental value due to strain gauges

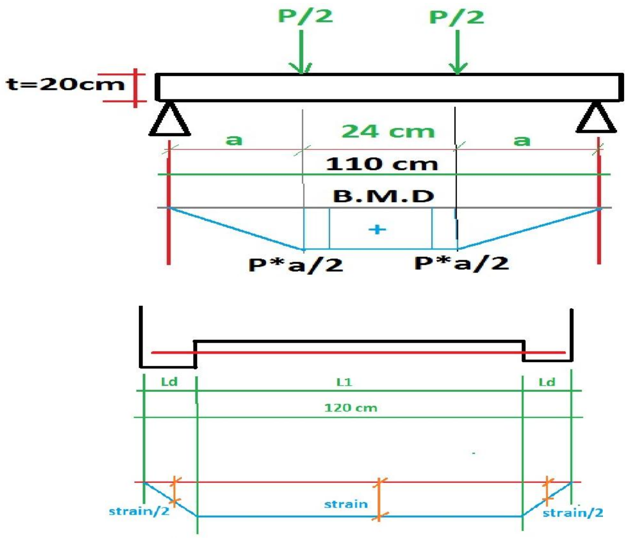

Fig.16. B.M.D and distribution on the beam

Table 5: Bond stress-Slippage of tested beams

Beam	NC or FC	Bar Surface	Bar	L_d mm	τ MPa	Slippage mm	τ G.F/ τ S	S G.F/ S S
B1	NC	Mechanical	GFRP	100	4.22	4.43	0.55	0.68
B2	NC	Spiral	GFRP	100	3.42	8.4	0.44	1.30
B3	FC	Sanded	GFRP	250	3.83	5.9	0.89	0.81
B5	NC	Mechanical	GFRP	250	5.7	3.4	1.32	0.46
B6	NC	Sanded	GFRP	100	1.83	7.6	0.23	1.16
B7	NC	Sanded	GFRP	200	3.2	4.16	0.42	0.64
B10	NC	notched	Steel	250	4.3	7.24	1	1
B15	NC	Spiral	GFRP	250	4.45	9.05	1.03	1.25
B16	FC	Sanded	GFRP	100	2.73	2.3	0.35	0.35
B17	FC	notched	Steel	250	1.65	1.7	0.38	0.23

τ G.F / τ S **Ratio Bond Stress**

S G.F / **S** S **Ratio slippage**
τ G.F **Bond stress of beam reinforced with GFRP bar**
τ S **Bond stress of beam reinforced with Steel bar**
S G.F **Slippage of beam reinforced with GFRP bar**
S S **Slippage of beam reinforced with Steel bar**

4.4 Bond-Slippage for Normal Concrete and Fiber Concrete

The average bond-slip experimental behavior of the two specimens of B6 and B7 is drawn on Fig. 17; the two specimens have failed in bond at bond stress of about 1.83 and 3.2 MPa respectively with corresponding slip between 7.6 and 4.16 mm respectively. The ratio of bond stress for GFRP bar (Nc-sanded treatment) to bond stress for Steel bar (τ G.F / τ S) is enhanced for specimen B7 compared to specimen B6 and reached 42% with increasing embedded length to 250 mm but not sufficient to reach the optimum bond strength for steel bar. As shown in Figs. 18, 19 and table 5, for both mechanical (B5) and spiral treatment (B15), the bond stress for GFRP bar are higher than that of deformed steel specimen by about 32% and 3% respectively, with corresponding ratio of slippage (**S** G.F **/ S** S **),** 0.46 and 1.25 respectively. For embedded length 100 mm, the specimens failed in bond failure, and the ratio of bond stress (τ G.F / τ S) reached up to 55%. As shown in Fig. (20), the fiber concrete has a negative impact on the bond strength increase, due to probability of existence voids in the fiber concrete.

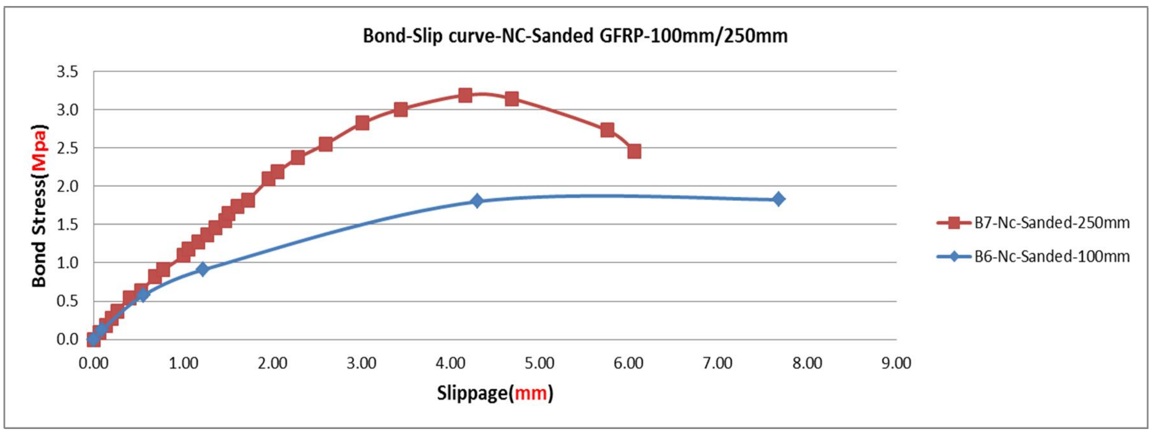

Fig.17. Bond-slip relations of GFRP beam B6 and B7

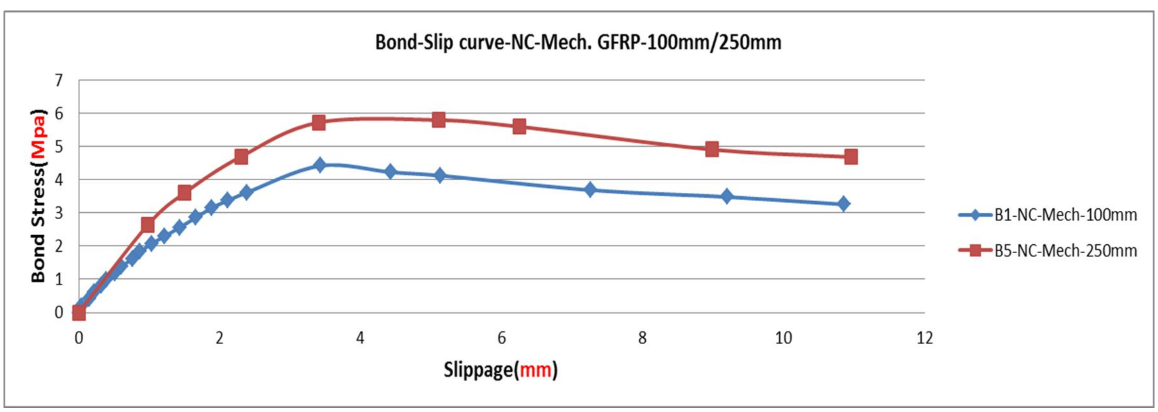

Fig.18. Bond-slip relations of GFRP beam B1 and B5

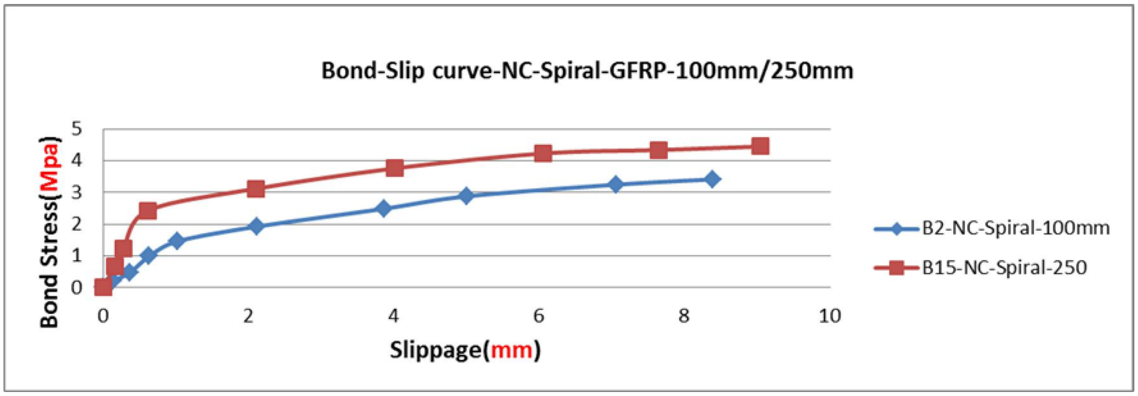

Fig.19. Bond-slip relations of GFRP beam B2 and B15

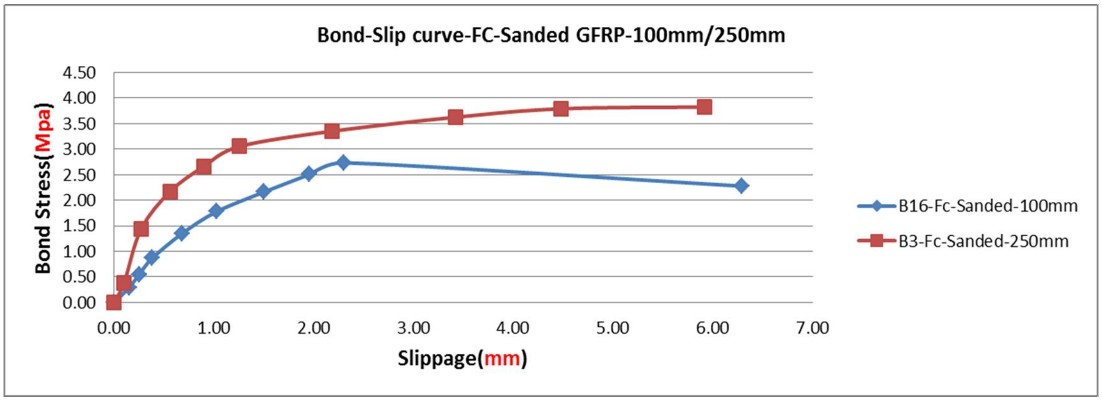

Fig.20. Bond-slip relations of GFRP beam B16 and B3

The average experimental bond-slip behavior of the GFRP for different treatment of bar end, and steel beam specimens with embedded length 250 mm is drawn in Fig. 21. Bond resistance of GFRP beam specimen B7 (3.2 MPa) and B3 (3.83 MPa) is found to be lower than that of deformed steel specimen B10 (4.3 MPa) by about 25 %, and 10% respectively, the fiber concrete effect increased the bond resistance Provided that the quality mixing of concrete. While, bond resistance of deformed steel specimen is found to be lower than the bond resistance of GFRP beams B15 (4.45 Mpa), and B5(5.7 Mpa) by about 3% and 30 % respectively. The mechanical treatment is more effective in enhanced the bond resistance. On the other hand the ultimate slip of GFRP specimen B5 is lower than that of deformed steel by 45%, and the ultimate slip of GFRP specimen B15 is larger than that of deformed steel specimen by about 25 %. The initial bond stiffness of GFRP specimens is lower of the deformed steel initial bond stiffness.

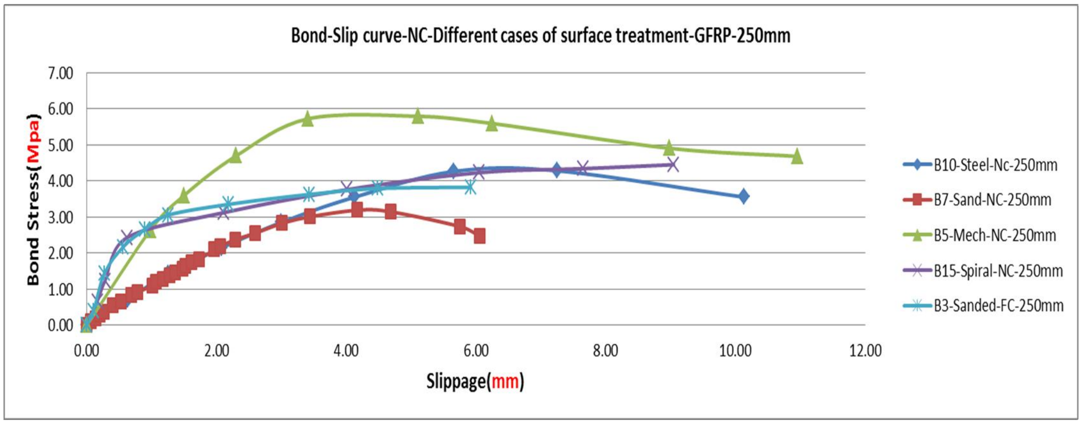

Fig.21. Bond-slip relations of GFRP beam B10, B7, B5 and Steel beam B15

5. Conclusion

In this paper an experimental program is design to investigate the bond-slip behavior between concrete and glass fiber reinforced polymer (GFRP) reinforcing bars under static loading. 19 Beam specimens reinforced with glass fiber (GFRP) bars, and steel bars are fabricated and tested. Beam specimens are tested under the specification specified four-point bending test. From the analysis and discussion of the test results the following conclusions can be obtained:

1. Initial slope (bond stiffness) bond-slip of GFRP specimens is lower than that of the notched steel specimens.
2. Bond resistance of GFRP beam specimen with sand treatment is lower than that of deformed steel specimen by about 25 %.
3. The fiber concrete has small effect (15% increase) in enhanced the bond resistance for the sanded GFRP treatment.
4. The bond resistance of GFRP beams with spiral treatment, and mechanical treatment is larger than bond resistance of deformed steel specimen by about 3% and 30 % of the bond resistance of deformed steel specimen.
5. The mechanical treatment is more effective in increasing the bond resistance than the spiral treatment.
6. The ultimate slip of GFRP specimen mechanical treatment is lower than that of deformed steel by 45%, and the ultimate slip of GFRP specimen spiral treatment is larger than that of deformed steel specimen by about 25 %.

6. References

1. Almusallam TH. Analytical prediction of flexural behavior of concrete beams reinforced by fibre reinforced polymer (FRP) bars. J Compos Mater 1997;31(7):640–57.
2. Cheung MS, Wiseman A. Development of Canadian standard for building construction using FRP composites. In: Proceeding of the 3rd International Conference on Advanced Composite Materials in Bridges and Structures, August 2000; Ottawa, Canada, 2000. p. 841–8.
3. Faza SS, GangaRao HVS. Theoretical and experimental correlation of behavior of concrete beams reinforced with fibre reinforced plastic rebars. In: Reinforced-plastic reinforcement for concrete structures, SP-138. Detroit: American Concrete Institute; 1993. p. 599–614.
4. Husain, M., "Experimental bond-slip behavior of FRP bars and concrete", American society of civil Engineers, 6th International Engineering and Construction Conference (IECC'6), Cairo, Egypt, June 28-30, 2010.
5. Masmoudi R, Theriault M, Benmokrane B. Flexural behavior of concrete beams reinforced with deformed fibre reinforced plastic reinforcing rods. ACI Struct J 1998;95(6):665–76.
6. Gentry, T. R. and Husain, M., "Thermal Compatibility of Concrete and Composite Reinforcement: Analytical and Numerical Predictions", Proceedings of First International Conference on Durability of FRP Composites for Construction, 1998, Sherbrooke, Quebec, Canada.
7. Gentry, T. R. and Husain, M., "Thermal Compatibility of Concrete and Composite Reinforcements", ASCE, Journal of Composites for Construction, May 1999, Vol. 3, Issue 2, pp. 82-86.
8. ACI 440. 1R-06, "Guide for the Design and Construction of Structural Concrete Reinforced with FRP Bars", American Concrete Institute, Detroit, Michigan, USA, 2006.
9. ACI 440. 3R-04, "Prestressing Concrete with FRP Tendons", American Concrete Institute, Detroit, Michigan, USA, 2004.
10. ACI 440. 4R-04, "Guide Test Methods for Fiber Reinforced Polymers (FRPs) for Reinforcing and Strengthening Concrete Structures", American Concrete Institute, Detroit, Michigan, USA, 2004.
11. Cho, J-R., Park, S. Y., Cho, K., Kim, S-T. and Kim, B-S, "Performance of Coarse Sand Coating between FRP member and Concrete", Proceedings of the eighth International Symposium on FRP-Reinforced Concrete Structures, FRPRCS-8, Patras, Greece, July 16-18, 2007.
12. Harajli, M. H., "Numerical Bond Analysis Using Experimentally Derived Local Bond Laws: A Powerful Method for Evaluating the Bond Strength of Steel Bars", ASCE, J. Struct. Engrg, V.133, Issue 5 (May 2007), 695-705.
13. Vogel, H. and Svecova, D., "Thermal Compatibility and Bond Strength of FRP Reinforcement in Prestressed Concrete Applications", (2007) ASCE, J. Composites for Construction, V11, Issue 5, 459-468.
14. Wambeke, B., and Shield, C., "Development Length of Glass Fiber-Reinforced Polymer Bars in Concrete", (2006) ACI Structural Journal V. 103, No. 1, Jan-Feb, pp. 11-17.
15. Safaan. M., 2004,"Mechanical Properties of Locally Produced GFRP Bars as Concrete Reinforcement", International conference: Future Vision and Challenges for Urban Development, HBRC Journal, Vol.1,No.1,20-22Dec.2004,ISSN12478/2004,Cairo,Egypt,pp.1-13
16. Gopalaratnam, V.S., and Meyer, J. W., "Fatigue Response of Flexural Bond in FRP Reinforced Concrete", ICFRC, Jan, 2004, India.
17. Tighiouart, B. Benmokrane, B., and Gao, D.(1998), "Investigation of bond in concrete member with fiber reinforced polymer (FRP) bars", Construction and Building Materials 12 (1998) pp453-462.
18. H. K. Shehab Eldin, M. M. Hussein, K.F. Khalil, Shady Khairy "Pullout bond behavior of GFRP bars and concrete", Journal of Al Azhar University Engineering Sector (JAUES), ISSN: 1110-6409, Cairo, Egypt, August 2013.
19. Benmokrane, B.; Masmoudi, R.; and El-Salakawy, E., 2004, "Designing and Testing of Concrete Bridges Deck Reinforced with Glass FRP Bars", SAMPE 2004-Long Beach, USA.

6/25/2014